

## MINERALOGICAL STUDY OF A NEW LUNAR METEORITE YAMATO 981031

T. Arai<sup>1</sup>, T. Ishi<sup>2</sup> and M. Otsuki<sup>2</sup>. <sup>1</sup>Space Station Mission Operations Department, Office of Space Utilization Systems, National Space Development Agency of Japan (NASDA), Tsukuba Space Center 2-1-1 Sengen Tsukuba, Ibaraki 305-8505 Japan, [arai.tomoko@nasda.go.jp](mailto:arai.tomoko@nasda.go.jp). <sup>2</sup>Ocean Research Institute, University of Tokyo, 1-15-1, Minamidai, Nakano-ku, Tokyo 164-8639 Japan.

**Introduction:** Lunar meteorites are valuable sources of information about crustal evolution of the Moon, in addition to Apollo/Luna samples which cover only limited regions of central nearside [1]. Yamato (Y) 981031 is the 7th Antarctic lunar meteorite of mare origin. Among the six pre-found mare meteorites, Yamato (Y) 793169 and Asuka (A) 881757 (YA) are unbrecciated mare basalts [e.g. 2, 3, 4], while Y 793274, QUE 94281, EET 87521, and EET96008 are brecciated mare basalts with some highland components. Y 793274 /QUE94281 (YQ) and EET87521 / EET96008 (EETs) are respectively derived from a common source crater [e.g. 5, 6]. In this study, mineralogy of Y981031 is investigated to identify its source mare-basalt suite and to assess its genetic relationship with other mare lunar meteorites.

**Sample and Methods:** The polished thin section (PTS) 981031, 53-4 is provided by the National Institute of Polar Research. Analyses of mineral compositions and chemical mapping were done by a JEOL 733 electron probe microanalyzer (EPMA) and JEOL EPMA (8900 Super Probe) at the Ocean Research Institute, University of Tokyo.

**Results:** Y981031 is a polymict, regolith breccia and is a diverse mixture of mineral fragments and clasts from various rock types. Mineral fragments, 100-500  $\mu\text{m}$  in size, are mostly pyroxene, plagioclase and olivine of apparent mare-basalt derivation, with fragments of minor opaque mineral, such as ilmenite, chromite, and silica minerals. These mineral fragments are scattered in a dark, glassy matrix. One big pyroxene fragment, 2.0 mm across is zoned from pigeonite to augite with symplectite of fayalite and silica mineral is found. Exsolution of about 1  $\mu\text{m}$  wide is noted.

This rock contains a variety of clasts, such as dark melt clasts, fine-grained anorthositic highland clasts, clast-poor impact melt clasts, mare basalt clasts, and a Mg-rich dunite clast. One dark melt clast is 3 mm across and a clast-poor impact melt clast, 3.5 mm across, includes dendritic plagioclase crystals.

The Mg-rich dunite clast (DN), 750  $\mu\text{m}$  across, is apparently an olivine-cumulate and consists of dominantly Mg-rich olivine with minor plagioclase and Mg-rich high-Ca pyroxene. The modal abundance in vol. % is: olivine (Fo90) = 88, plagioclase (An88-90) = 9, and high-Ca pyroxene (Wo48En48Fs6, Fe/Fe+Mg = 0.9) = 3. The high-Ca pyroxenes are plotted in pyroxene quadrilateral and Fe# (=Fe/(Fe+Mg) molar) vs. Ti# (=Ti/(Ti+Cr) molar) diagram (Fig. 2 and 3). The DN clast is clast represents a rare rock type, a Mg-rich dunite. The modal abundance and mineral composition are analogous to an Apollo 17 sample, 72415 [7]. This clast is apparently exotic compared with mare component and anorthositic highland component.

The coarse-grained (1 mm-size pyroxene) mare basalt clasts (MB) and associated mare pyroxene fragments are clustered in one corner of the thin section (Fig. 1a). The basalt clasts, 0.5 – 1 mm in size, are composed of zoned pyroxenes from pigeonite to augite, plagioclase (An85-96),

with mesostases including fayalite (Fo17-19), ilmenite, chromian ulvöspinel (Chr3Her12Ulvo81-Chr32Her12Ulvo56), and troilite. The composition of chromian ulvöspinel is close to that of A881757 [6]. The pyroxenes compositions are depicted in pyroxene quadrilateral and Fe# vs. Ti# plot (Fig. 2 and Fig. 3). The MB pyroxenes constitute a series of trend in the Fe# vs. Ti# plot, which is typical of zoned pyroxenes in the Ti-poor mare basalt, and the trend is slightly more steep and Ti-rich than that of YQ and EET meteorites [5, 6]. Although the most primitive composition of MB pyroxenes is more Mg-rich than YA basalts [8], the compositional trend in Fe# vs. Ti# is partly analogous to those of YA meteorites [8].

Based on an empirical correlation between Ti# in pyroxene and bulk-rock TiO<sub>2</sub> abundance [5], a source basalt of MB pyroxenes is estimated to have a bulk-rock TiO<sub>2</sub> = 1.3 – 1.5 wt %, which falls between YQ/EET basalts (TiO<sub>2</sub> = 1.0 wt %) [5, 6] and YA basalts (TiO<sub>2</sub> = 1.5 - 2.0 wt%) [e.g. 2].

Mare pyroxenes from MB clasts and fragments in the matrix commonly feature about 1  $\mu\text{m}$ -wide exsolution.

The Y981031 contains glass spherules and spherule fragments. Pale-green glasses are larger (100 - 600  $\mu\text{m}$  across) and mostly spherule fragments (Fig. 1b). Smaller, colorless glass spherules are 50-100  $\mu\text{m}$  in diameter (Fig. 1b). Some glasses show inclusions and schlieren, which are indicators of impact origin [9]. The pale-green glass of 600  $\mu\text{m}$  in size contains a mineral assemblage of pyroxene and plagioclase (150  $\mu\text{m}$ ). The both types of glasses show homogeneous composition within each glass, while slightly compositional variation between glasses are found. Average compositions for the glasses are shown in Table 1. Compared with the pale-green glasses, the clear glasses show higher Al<sub>2</sub>O<sub>3</sub> and lower MgO, except one clear glass (CL1). The Aluminum-rich glasses are probably of impact origin, while others are pyroclastic glasses. However, the volcanic origin of PG1, 2, and 3 is enigmatic, because of their lower Mg/Al = 0.7-0.9. Based on the criteria of Delano (1986) [9], Mg/Al is one indicator to distinguish pyroclastic glass (> 1.5) from impact glass (< 1.5). Pale-green glasses and colorless spherules are also found in YQ meteorites [5]. Note that the composition of the both type of glasses in Y981031 is within a same range of YQ glass composition.

A light brown fusion crust (0.2 - 0.3 mm thick) is found with abundant vesicles in it. The fusion crust shows relatively homogeneous composition and the average composition is shown in Table 1.

**Discussion:** The overall texture, dark glassy matrix, the presence and compositional similarity of pyroclastic/impact glasses suggests close genetic relation of Y981031 with YQ meteorites [5], possibly derived from a common source crater. The coarse exsolution feature of pyroxene (around 1  $\mu\text{m}$  in width) by mare standard is also consistently recognized in all the Antarctic lunar mare brecciated meteorites found so far [5,6,8]. This indicates that mare-basalt remnants (mainly

Mineralogical Study of A New Lunar Meteorite Yamato 981031: T. Arai *et al.*

pyroxene) in these lunar mare breccias preserve a common cooling process, implying that their source basalt experienced relatively slow cooling, such as relatively slow-cooling in a thick lava flow or lava pond.

The Y981031 has also some common features with YA meteorites which are an unbrecciated mare basalt [e.g. 10]. The MB clasts show very similar mineral assemblage/composition and coarse-grained basalt texture to that of YA meteorites [8]. Although the most primitive composition of MB pyroxenes is more Mg-rich than that of YA meteorites, Ti# variation trend with increasing Fe# is similar to YA meteorites. It is noted that the MB mesostases consists of almost identical mineral assemblage and composition of the chromian ulvöspinel to that of A881757 [8]. A881757 basalt and Y981031 commonly contains symplectic pyroxenes that were probably produced by shock metamorphism. These facts imply that mare basalt components in Y981031 and YA meteorites, especially A881757 might have cooled from a similar (in composition) lava flow and have experienced a similar secondary shock events, possibly an impact to the commonly cooled lava flow.

**Conclusions:** Commonality in the overall texture, the presence and composition of pyroclastic/impact glasses suggests "source-crater pairing" of Y981031 and YQ meteorites. Similarity of pyroxene zoning trend, presence of symplectic pyroxene, mesostases mineral assemblages/mineral compositions in the mare basalt component, and source-basalt TiO<sub>2</sub> implies "source-basalt pairing" of Y981031 and YA meteorites.

**Acknowledgements-**The authors thank NIPR for allocating the sample.

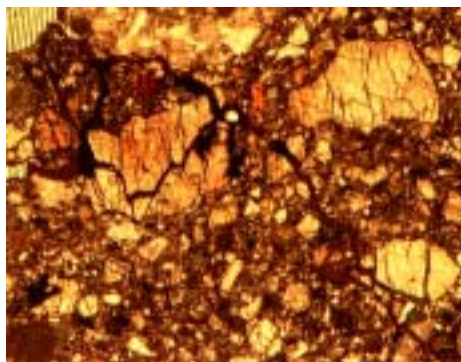


Fig.1a Photomicrograph of MB clasts (3.3 mm across)

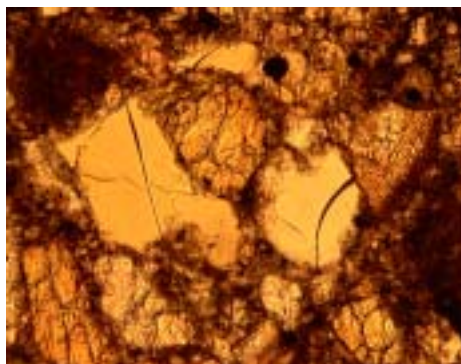


Fig.1b Photomicrograph of a pale-green glass spherule (left) and a colorless spherule fragment (right) (0.7 mm across).

**References:** [1] Feldman W. C. et al. (1998) *LPS* **29**, abstract #1936. [2] Yanai K. & Kojima H. (1991) *Proc. NIPR Ant. Met.* **4**, 70-90. [3] Warren P. H. & Kallemeyn G. W. (1993) *Proc. NIPR Ant. Met.* **6**, 35-57. [4] Takeda H. et al. (1993) *Proc. NIPR Ant. Met.* **6**, 3-13. [5] Arai T. & Warren P. H. (1999) *MPS*, **34**, 209-234. [6] Arai T. (2001) *Antarctic Meteorites XXVI*, 2-6. [7] Taylor G. J. et al. (1991) *Lunar Sourcebook*, pp.183-284, Cambridge U. Press. [8] Arai T et al. (1996) *MPS*, **31**, 877-892. [9] Delano J.W. (1986) *Proc. LPSC*, **16**, D201-D213. [10] Yanai K. (1991) *PLPS* **21**, 314-324.

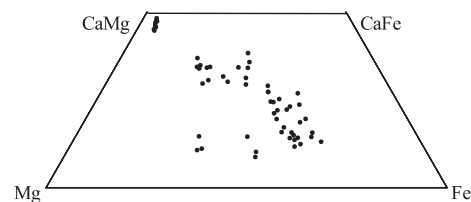


Fig.2 Pyroxene from DN and MB clasts are plotted in pyroxene quadrilateral. DN pyroxenes are clustered at the Mg-rich and Ca-rich corner.

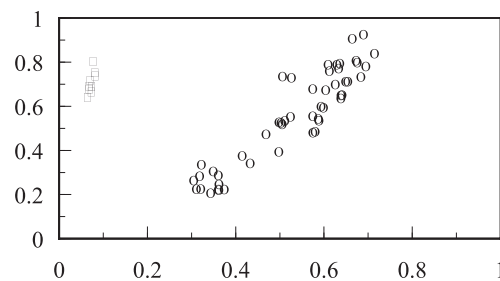


Fig.3 Fe# vs. Ti# plot for MB and DN pyroxenes. Open circle for MB pyroxene and open square for DN pyroxenes.

Table 1 Chemical compositions of pale-green glass (PG), colorless glasses (CL), and fusion crust (FC).

	PG1	PG2	PG3	CL1	CL2	CL3	CL4	FC
SiO <sub>2</sub>	47.7	48.4	47.7	45.9	42.8	45.2	39.9	45.7
TiO <sub>2</sub>	1.5	1.3	1.0	0.5	0.3	0.4	0.5	0.7
Al <sub>2</sub> O <sub>3</sub>	11.4	11.5	12.3	9.7	30.4	22.2	27.9	17.0
FeO	18.6	18.4	16.9	17.9	3.7	9.3	6.8	13.2
MnO	0.3	0.3	0.2	0.2	0.1	0.1	0.1	0.2
MgO	6.5	6.7	8.6	14.3	4.8	7.4	8.0	9.8
CaO	12.0	12.1	11.8	9.5	17.8	14.1	16.7	12.1
Na <sub>2</sub> O	0.4	0.3	0.4	0.3	0.2	0.1	0.0	0.4
Cr <sub>2</sub> O <sub>3</sub>	0.2	0.2	0.3	0.5	0.1	0.2	0.1	0.2
Total	98.5	99.2	99.1	98.8	100.1	99.1	100.0	99.3
Mg/Al	0.7	0.7	0.9	1.9	0.2	0.4	0.4	0.7